



1 **Unexpected enhancement of ozone exposure and health risks during National Day in China**

2 Peng Wang^{1,2}, Juanyong Shen³, Men Xia¹, Shida Sun⁴, Yanli Zhang², Hongliang Zhang^{5,6}, Xinming Wang²

3 ¹Department of Civil and Environmental Engineering, The Hong Kong Polytechnic University, Hong Kong,
4 China

5 ²State Key Laboratory of Organic Geochemistry and Guangdong Key Laboratory of Environmental
6 Protection and Resources Utilization, Guangzhou Institute of Geochemistry, Chinese Academy of Sciences,
7 Guangzhou, China

8 ³School of Environmental Science and Engineering, Shanghai Jiao Tong University, Shanghai, China

9 ⁴Tianjin Key Laboratory of Urban Transport Emission Research, College of Environmental Science and
10 Engineering, Nankai University, Tianjin, China

11 ⁵Department of Environmental Science and Engineering, Fudan University, Shanghai, China

12 ⁶Institute of Eco-Chongming (IEC), Shanghai, China

13 *Correspondence to:* Yanli Zhang (zhang_y186@gig.ac.cn)

14

15 **Abstract**

16 China is confronting increasing ozone (O₃) pollution that worsens air quality and public health. Extremely
17 O₃ pollution occurs more frequently under special events and unfavorable meteorological conditions. Here
18 we observed significantly elevated maximum daily 8-h average (MDA8) O₃ (up to 98 ppb) during the
19 Chinese National Day Holidays (CNDH) in 2018 throughout China, with a prominent rise by up to 120%
20 compared to the previous week. Air quality model shows that increased precursor emissions and regional
21 transport are major contributors to the elevation. In the Pearl River Delta region, the regional transport
22 contributed up to 30 ppb O₃ during the CNDH. Simultaneously, aggravated health risk occurs due to high
23 O₃, inducing 33% additional deaths throughout China. Moreover, in tourist cities such as Sanya, daily
24 mortality even increases by up to 303%. This is the first comprehensive study to investigate O₃ pollution
25 during CNDH at national level, aiming to arouse more focuses of the O₃ holiday impact from the public.

26

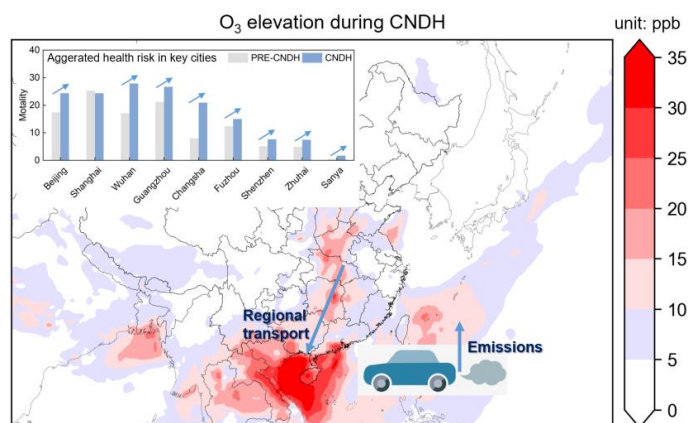
27

28

29



30 Graphical abstract



32 1. Introduction

33 Tropospheric ozone (O₃) has become a major air pollutant in China especially in urban areas such as
34 the North China Plain (NCP), Yangtze River Delta (YRD) and Pearl River Delta (PRD) in recent years,
35 with continuously increasing maximum daily 8-h average (MDA8) O₃ levels (Fang et al., 2019;Li et al.,
36 2019;Lu et al., 2018;Liu et al., 2018a). Exacerbated O₃ pollution aggravates health risks from a series of
37 illnesses such as cardiovascular diseases (CVD), respiratory diseases (RD), hypertension, stroke and
38 chronic obstructive pulmonary disease (COPD) (Liu et al., 2018a;Li et al., 2015;Brauer et al.,
39 2016;Lelieveld et al., 2013;Wang et al., 2020b). In China, the annual COPD mortality due to O₃ reaches up
40 to 8.03×10^4 in 2015 (Liu et al., 2018a).

41 O₃ is generated by non-linear photochemical reactions of its precursors involving volatile organic
42 compounds (VOCs) and nitrogen oxides (NO_x) (Sillman, 1995;Wang et al., 2017). The VOCs/NO_x ratio
43 determines O₃ sensitivity that is classified as VOC-limited, transition and NO_x-limited, which controls O₃
44 formation (Sillman, 1995;Sillman and He, 2002;Cohan et al., 2005). Also, regional transport was reported
45 as an important source of high O₃ in China (Gao et al., 2016;Wang et al., 2020a;Li et al., 2012a). For
46 instance, Li et al. (2012b) showed that over 50% of surface O₃ was contributed from regional transport in
47 the PRD during high O₃ episodes.

48 O₃ concentration shows different patterns between holidays and workdays (Pudasainee et al., 2010;Xu
49 et al., 2017). Elevated O₃ has been observed during holidays in different regions resulted from changes in
50 precursor emissions related to intensive anthropogenic activities (Tan et al., 2009;Chen et al., 2019;Tan et
51 al., 2013;Levy, 2013). In China, most studies focused on the Chinese New Year (CNY) to investigate long-
52 term holiday effect on O₃ in southern areas (Chen et al., 2019). However, the Chinese National Day



53 Holidays (CNDH), a nationwide 7-day festival, is less concerned. Xu et al. (2017) reported that the O₃
54 production was influenced by enhanced VOCs during CNDH in the YRD based on in-situ observations.
55 Previous studies mainly paid attention to developed regions/cities without nationwide consideration. In
56 addition, the national O₃-attributable health impact during CNDH is also unclear. Consequently, a
57 comprehensive study on O₃ during the CNDH is urgently needed in China.

58 In this study, we used observation data and a source-oriented version of the Community Multiscale
59 Air Quality (CMAQ) model (Wang et al., 2019a) to investigate O₃ characteristics during the CNDH in 2018
60 in China. Daily premature death mortality was evaluated to determine health impacts attributed to O₃ as
61 well. We find a rapid increase by up to 120% of the observational MDA8 O₃ from previous periods to
62 CNDH throughout China, which is attributed to increased precursors and regional transport. This study
63 provides in-depth investigation of elevated O₃ and its adverse health impacts during CNDH, which has
64 important implications for developing effective control policies in China.

65 2. Methods

66 2.1 The CMAQ model setup and validation

67 The CMAQ model with three-regime (3R) that attributed O₃ to NO_x and VOCs based on the NO_x-
68 VOC-O₃ sensitivity regime was applied to study the O₃ during CNDH in China in 2018. The regime
69 indicator R was calculated using Eq. (1):

$$R = \frac{P_{H_2O_2} + P_{ROOH}}{P_{HNO_3}} \quad (1)$$

70 where $P_{H_2O_2}$ is the formation rate of hydrogen peroxide (H₂O₂); P_{ROOH} is the formation rate of organic
71 peroxide (ROOH), and P_{HNO_3} is the formation rate of nitric acid (HNO₃) in each chemistry time step. The
72 threshold values for the transition regime are 0.047 (R_{ts} , change from VOC-limited to transition regime)
73 and 5.142 (R_{te} , change from transition regime to NO_x-limited regime) in this study (Wang et al., 2019b).
74 The formed O₃ is entirely attributed to NO_x or VOC sources, when R values are located in NO_x-limited
75 ($R > R_{te}$) or VOC-limited ($R < R_{ts}$) regime. In contrast, when R values are in the transition regime
76 ($R_{ts} \leq R \leq R_{te}$), the formed O₃ is attributed to both NO_x and VOC sources. Two non-reactive O₃ species:
77 O₃_NO_x and O₃_VOC are added in the CMAQ model to quantify the O₃ attributable to NO_x and VOCs,
78 respectively. The details of the 3R scheme are described in Wang et al. (2019b).

79 A domain with a horizontal resolution of 36×36 km² was applied in this study, covering China and its
80 surrounding areas (Fig. S1). Weather Research and Forecasting (WRF) model version 3.9.1 was used to
81 generate the meteorological inputs, and the initial and boundary conditions were based on the FNL
82 reanalysis data from the National Centers for Environmental Prediction (NCEP). The anthropogenic



83 emissions in China are from the Multiresolution Emission Inventory for China (MEIC,
84 <http://www.meicmodel.org/>) version 1.3 that lumped to 5 sectors: agriculture, industries, residential,
85 power plants, and transportation. The monthly profile of the anthropogenic emissions was based on
86 Zhang et al. (2007) and Streets et al. (2003) as shown in Table S1 to represent the emissions changes
87 between September and October. Emissions from other countries were from MIX Asian emission
88 inventory (Li et al., 2017). Open burning emissions were from the Fire INventory from NCAR (FINN)
89 (Wiedinmyer et al., 2011), and biogenic emissions are generated using the Model of Emissions of Gases
90 and Aerosols from Nature version 2.1 (MEGAN2.1) (Guenther et al., 2012). The Integrated Process Rate
91 (IPR) in the Process Analysis (PA) tool in the CMAQ model was applied to quantify the contributions of
92 atmospheric processes to O₃ (Gipson, 1999) (details see Table S2).

93 The simulation period was from 24 September to 31 October in 2018 and divided into three intervals:
94 PRE-CNDH (24-30, September), CNDH (1-7, October) and AFT-CNDH (8-31, October). In this study, a
95 total of 43 cities that includes both megacities (such as Beijing and Shanghai) and popular tourist cities
96 (such as Sanya) were selected to investigate the O₃ issue during CNDH in 2018 in China (Table S3).
97 Locations of these cities cover developed (such as the YRD region) and also suburban/rural regions (such
98 as Urumqi and Lhasa in western China), which provides comprehensive perspectives for this study (Fig.
99 S1).

100 All the statistics results of the WRF model are satisfied with the benchmarks except for the GE of
101 temperature (T2) and wind speed (WD) went beyond the benchmark by 25% and 46%, respectively (Table
102 S4). The WRF model performance is similar to previous studies (Zhang et al., 2012; Hu et al., 2016) that
103 could provide robust meteorological inputs to the CMAQ model. The observation data of key pollutants
104 obtained from the national air quality monitoring network (<https://quotsoft.net/air/>, more than 1500 sites)
105 were used to validate the CMAQ model performance. The model performance of O₃ was within the criteria
106 with a slight underestimation compared to observations, demonstrating our simulation is capable of the O₃
107 study in China (Table S5).

108

109 **2.2 Health impact estimation**

110 The daily premature mortalities due to O₃ from all non-accidental causes, CVD, RD, hypertension,
111 stroke and COPD are estimated in this study. The O₃-related daily mortality is calculated based on
112 Anenberg et al. (2010) and Cohen et al. (2004). In this study, the population data are from all age groups,
113 which may induce higher daily mortality than expected (Liu et al., 2018a). In this study, the daily
114 premature mortality due to O₃ is calculated from the following Eq. (2) (Anenberg et al., 2010; Cohen et
115 al., 2004) :

116

$$\Delta M = y_0 [1 - \exp(-\beta \Delta X)] Pop \quad (2)$$



117 where ΔM is the daily premature mortality due to O_3 ; y_0 is the daily baseline mortality rate, collected from
118 the China Health Statistical Yearbook 2018 (National, 2018); β is the concentration-response function
119 (CRF), which represents the increase in daily mortality with each $10 \mu\text{g m}^{-3}$ increase of MDA8 O_3
120 concentration, cited from Yin et al. (2017); ΔX is the incremental concentration of O_3 based on the threshold
121 concentration (35.1 ppb) (Lim et al., 2012; Liu et al., 2018a); Pop is the population exposure to O_3 , obtained
122 from China's Sixth Census data (Fig. S2) (National Bureau of Statistics of China, 2010). The daily y_0 and
123 β values for all non-accidental causes, CVD, RD, hypertension, stroke and COPD are summarized in Table
124 S6.

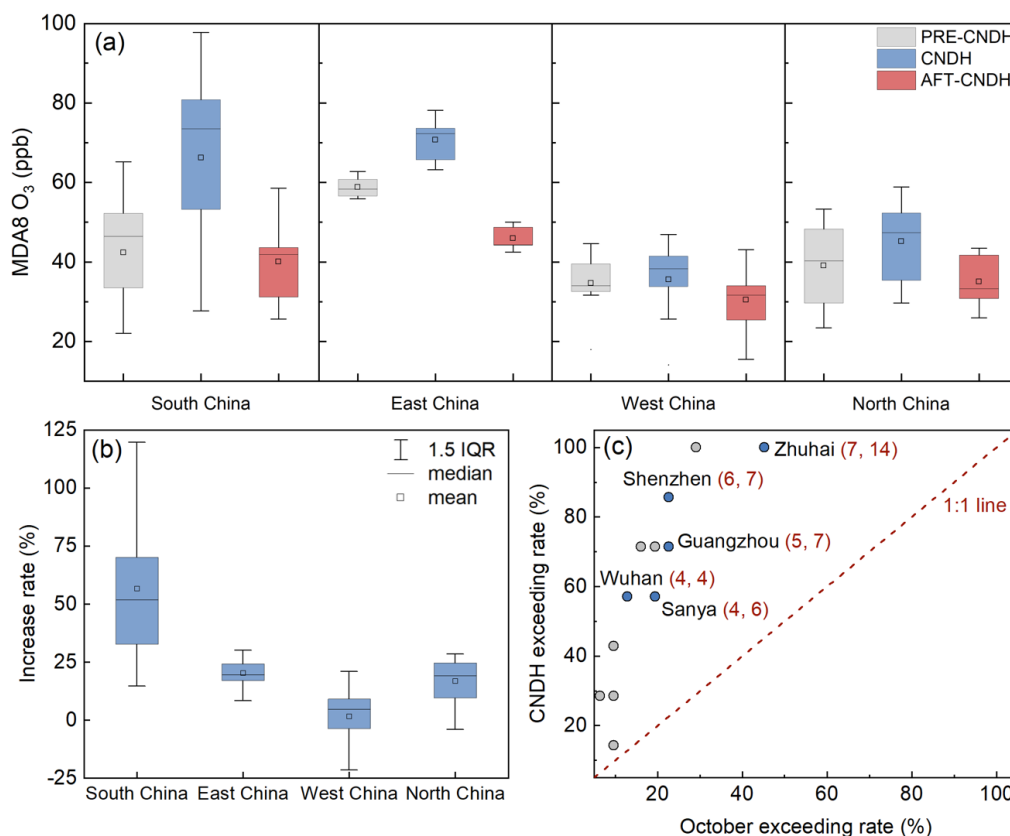
125

126 3. Results and Discussions

127 3.1 Observational O_3 in China during CNDH

128 MDA8 O_3 levels have noticeably risen during the 2018 CNDH based on observations, from 43 ppb
129 (PRE-CNDH) to 55 ppb (CNDH) among selected cities (Figure 1a and Table S3). The largest increase of
130 MDA8 O_3 (up to 56%) is observed in South China (Fig. 1b). The PRD region has recorded 49 % of MDA8
131 O_3 increase and in most PRD cities (such as Shenzhen and Guangzhou), number of exceeding days is as
132 high as 5~7 days during the 7-day CNDH, which contributed to 50 ~ 86% of days exceeding the Chinese
133 national air quality standards (Grade II, ~75 ppb) in the whole October (Fig. 1c). Other regions exhibit less
134 MDA8 O_3 increases, which are 20%, 16% and 3% for East, North and West China, respectively (Fig. 1b).
135 Negligible MDA8 O_3 increase in West China is consistent with vast rural areas and less anthropogenic
136 impacts. This result suggests that changes in anthropogenic emissions have significant impacts on MDA8
137 O_3 during the CNDH in the South, East, and North China, similar to a previous observation study (Xu et
138 al., 2017).

139 Nine key cities are then selected for analyzing the causes and impacts of the remarkable MDA8 O_3
140 rises. Comprehensive criteria were adopted in selection according to: (1) acute MDA8 O_3 increases (e.g.,
141 Changsha and Shenzhen), and (2) important provincial capitals (e.g., Beijing and Shanghai) and famous
142 tourist cities (e.g., Sanya). The selected key cities are delegates of broad regions in China except for West
143 China (Fig. S1) with insignificant MDA8 O_3 increase (Table S3) and fewer traveling cities. The MDA8 O_3
144 increased by 48 ± 37 % during the 2018 CNDH in these key cities. The highest MDA8 O_3 is observed in
145 Zhuhai, reaching 98 ppb on average with the peak of 107 ppb. The MDA8 O_3 in Sanya increases twofold
146 compared to PRE-CNDH. This is unexpected as Sanya is less-concerned regarding air pollution and known
147 for less anthropogenic emissions (Wang et al., 2015). Other key cities show 8-70% increases during the
148 CNDH. The exact causes of substantial O_3 increases in these cities are of high interest and explored below.



149

150 **Figure 1.** (a) The observed average MDA8 O₃ in PRE-CNDH, CNDH and AFT-CNDH in South, East,
 151 West and North China in 2018; (b) The increase rate of observed MDA8 O₃ during CNDH; (c) The
 152 exceeding rate of observed MDA8 O₃ in CNDH and October. Blue dots refer to the key cities and grey
 153 dots represent other cities. The pairs of values in the parentheses following city name are the exceeding
 154 days in CNDH and October, respectively. IQR is the interquartile range.

155

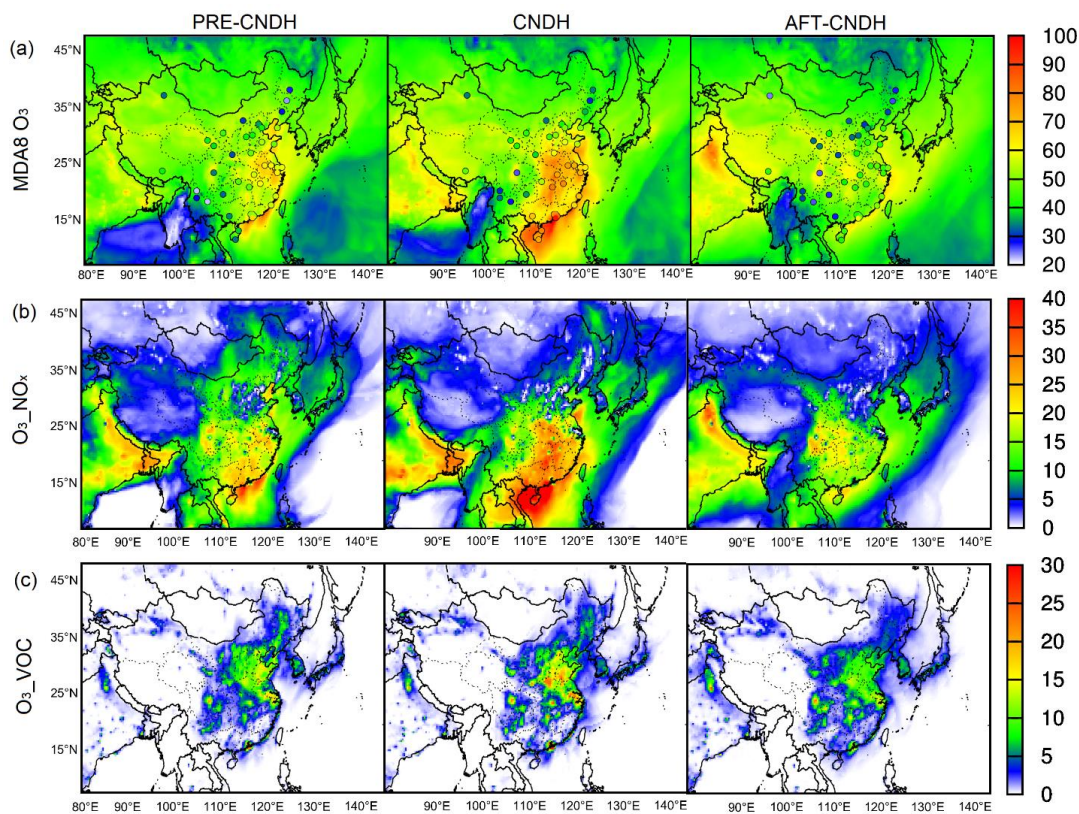
156 3.2 Increased O₃ precursor emissions during CNDH

157 The CMAQ is capable to represent the changes in observed MDA8 O₃ (Fig. 2). Generally, increasing
 158 trends of MDA8 O₃ are found in vast areas from PRE-CNDH to CNDH, suggesting the elevated O₃ occurs
 159 on a regional-scale. In South China, MDA8 O₃ reaches ~90 ppb that is approximately 1.2 times of the Class
 160 II standard with averaged increase rate of 30%. In contrast, the highest MDA8 O₃ drops sharply to 60 ppb
 161 in same regions in AFT-CNDH. High O₃-NO_x and O₃-VOC levels are also found during CNDH with
 162 different spatial distributions (Fig. 2). The rising O₃-NO_x areas are mainly located in South China covering



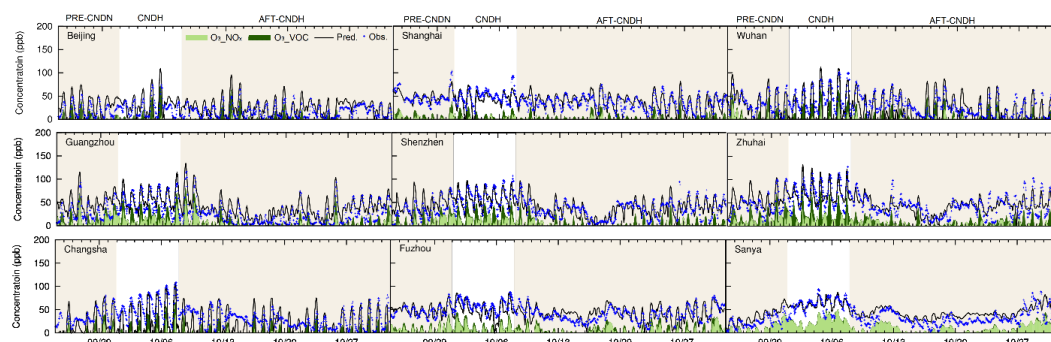
163 Hubei, Hunan, Guangxi, Jiangxi, north Guangdong and Fujian provinces with average increase of ~5-10
164 ppb. While high O_3_VOC regions are in developed city clusters such as the NCP, YRD and PRD regions.
165 In the PRD, peak O_3_VOC is over 30 ppb during the CNDH, which is 1.5 times of that in PRE-CNDH.
166 Similar to MDA8 O_3 , decreases in both $O_3_NO_x$ and O_3_VOC are found in AFT-CNDH. For the nine key
167 cities, $O_3_NO_x$ and O_3_VOC are also increased during CNDH. In Sanya, non-background O_3 during CNDH
168 is two times of that in PRE-AFDH. The peak of non-background O_3 ($O_3_NO_x + O_3_VOC$) is over 80 ppb
169 in Beijing and Zhuhai, indicating that O_3 formation plays an important role during CNDH (Fig. 3). In
170 megacities such as Beijing, O_3_VOC is the major contributor to elevated O_3 , while $O_3_NO_x$ becomes
171 significant in tourist cities such as Sanya.

172



173

174 **Figure 2.** (a) Comparison of observed (circle) and predicted MDA8 O_3 ; (b) Spatial distribution of $O_3_NO_x$;
175 (c) Spatial distribution of O_3_VOC in China in PRE-CNDH, CNDH and AFT-CNDH, respectively. Units
176 are ppb.



177

178 **Figure 3.** Hourly O₃ and its source apportionment results in nine key cities.

179 Considering O₃ sensitivity regimes (determined by equation (S1)), no noticeable differences are
180 observed between PRE-CNDH and CNDH (Fig. S3). During CNDH, the VOC-limited regions are mainly
181 in the NCP and YRD accompanied by high O₃_VOC. In South China, O₃ formation is under the transition
182 regime in most regions and NO_x-limited regions are in Fujian as well as part of Guangdong and Guangxi.
183 Increasing NO_x emissions are observed in Guangxi and Guangdong with relative increase of up to 100%
184 during CNDH, corresponding to rising O₃ in these NO_x-limited regions (Fig. S4). Simultaneously, higher
185 anthropogenic VOC emissions are observed during CNDH in South China, leading to elevated O₃ in the
186 transition regime when O₃ formation is controlled by both VOC and NO_x. In contrast, during AFT-CNDH,
187 more areas turn into transition regime in South China. The decreases in biogenic VOCs (compared to
188 CNDH) (Fig S4) due to temperature (Fig. S5) reduce MDA8 O₃ for regions in transition regime during
189 AFT-CNDH. Accordingly, changes in O₃ highly depends on its precursor emissions (NO_x and VOCs) as
190 well as the sensitivity regime.

191 Transportation increase due to tourism is also a potential source of elevated O₃ during holidays (Xu et
192 al., 2017). However, changes in transportation emissions are not considered in this study due to lack of
193 related statistical data. Residents prefer to travel during CNDH and thus more important impacts may be
194 from mobile sources (Zhao et al., 2019). Traveling by private cars is the most common approach, leading
195 to a significant increase in vehicle activities (Wang et al., 2019c). Time-varying coefficients are estimated
196 to describe traffic flow according to AMAP (2018) report during 2018 CNDH (Fig. S6). On average, CNDH
197 is 2.2 times the traffic flow of ordinary weeks. The heavy traffic flow occurs on October 1st (coefficient of
198 16.3%) and 5th (6.1%), due to intensive departure and return, respectively. Hourly variations of traffic flow
199 in CNDH are similar to weekends, having a flatter trend compared to workdays (Liu et al., 2018b). A real-
200 time vehicle emission inventory should be developed in future to better predict O₃ changes during CNDH.

201

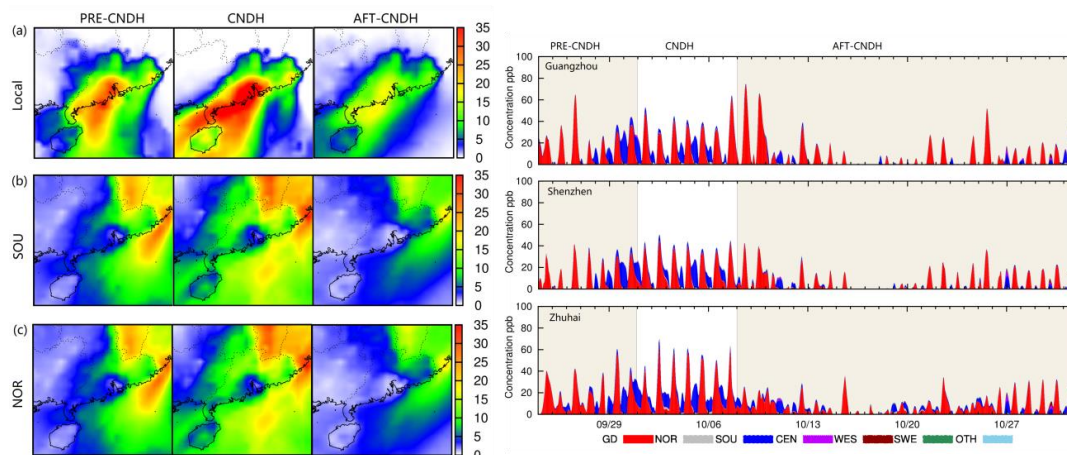


202 3.3 Impacts of regional Transport during CNDH

203 Regional transport is also a major contributor to enhanced MDA8 O₃ during CNDH. The higher O₃
204 production rates (increase rate up to ~150%) are observed mainly in the urban regions (the NCP, YRD, and
205 PRD) in China (Fig. S7). With north winds (Fig. S5), O₃ is transported from the north regions to downwind
206 South China to cause aggravated O₃. In the nine key cities, enhanced regional transport (HADV: horizontal
207 advection) of O₃ in Beijing, Changsha, Fuzhou, Shenzhen, Sanya, and Shanghai is as high as 90 ppb (Fig.
208 S8).

209 A regional-source tracking simulation was conducted in the PRD that occurred important O₃ elevation
210 to qualify the impacts of regional transport. The emissions were classified into 7 regional types (Fig. S9):
211 the local PRD (GD), northern part (NOR), southern part (SOU), central part (CEN), western part (WES),
212 southeast part (SWE) and other countries (OTH). The detailed model description could be found in Wang
213 et al. (2020a). Although the local sector contributes more than 50% non-background O₃ from PRE-CNDH
214 to AFT-CNDH the more significant O₃ regional transport are predicted during the late PRE-CHDH and
215 CNDH in the PRD, manifesting important role of the its important role in the O₃ elevation (Fig. 4 and S10).
216 The SOU sector is the most crucial contributors among all these regional sectors outside Guangdong due
217 to the prevailing south wind.

218 In these PRD key cities (Guangzhou, Shenzhen, and Zhuhai), the contribution of SOU sector in the
219 non-background O₃ is up to ~30 ppb, mainly occurring in the nighttime and early morning (Figure 4). In
220 the noontime, ~10-15% non-background O₃ is from SOU sector during the CNDH compared to less 5% in
221 other periods. The O₃_NO_x shows more significant regional transport characteristics than that of the
222 O₃_VOC (Fig. S11 and S12). During the late pre-CNDH and the CNDH, the contribution from regional
223 transport in the O₃_NO_x is up to 35 ppb. Due to the enhanced regional transport during the CNDH, the
224 O₃_NO_x could be even transported from the long-distance sector as NOR to the PRD. The peak of O₃_NO_x
225 due to the regional transport is predicted in the midnight, which is different of that of O₃_VOC (peak in the
226 noontime).



227

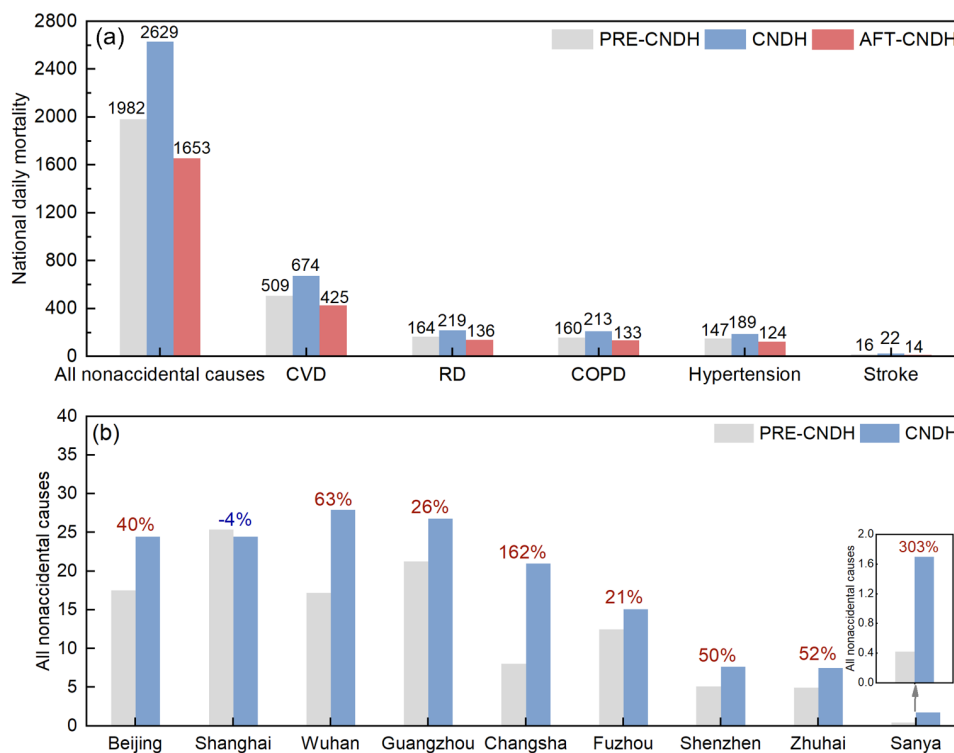
228 **Figure 4.** (a) Average regional contributions to non-background O₃ in from the PRD local emissions and
229 emissions in SOU, and NOR sectors and (b) regional contributions from all sectors to non-background O₃
230 in the PRD key cities (Guangzhou, Shenzhen, and Zhuhai) during the simulation periods.

231

232 3.4 Aggravated Health Risk during CNDH

233 It is recognized that O₃ pollution induces serious health risks from CVD, RD, COPD, hypertension
234 and stroke (Lelieveld et al., 2013; Yin et al., 2017; Huang et al., 2018; Krewski et al., 2009). Elevated MDA8
235 O₃ during CNDH leads to significantly higher health risks (Fig. 5). Estimated total national daily mortality
236 (from all non-accidental causes) due to MDA8 O₃ is 2629 during CNDH, 33% higher than that (1982) in
237 PRE-CNDH. All above O₃-related diseases have noticeable increases in national daily mortality during
238 CNDH. The highest health risk among these diseases is from CVD (674 during the CNDH), which is
239 consistent with Yin et al. (2017), followed by RD (219), COPD (213), hypertension (189) and stroke (22).
240 The COPD mortality due to O₃ in this study is comparable with 152-220 in Liu et al. (2018a). In AFT-
241 CNDH, total daily mortality (drops to 1653) and mortality from all diseases decreases due to substantial O₃
242 reduction. Also, a substantial increase in the total daily mortality is shown throughout China during the
243 CNDH especially at those densely-populated regions (e.g., the YRD and PRD) (Fig. S11), which is
244 consistent with previous studies (Chen et al., 2018; Liu et al., 2018a; Wang et al., 2020b).

245



246

247 **Figure 5.** (a) National daily mortality from all non-accidental causes, CVD, RD, COPD, hypertension and stroke
 248 attributed to O₃ in RRE-CNDH, CNDH and AFT-CNDH and (b) Daily mortality from all non-accidental causes
 249 due to O₃ in the 9 key cities. Red/blue values above the bars are the increase/decrease rates of daily mortality
 250 from PRE-CNDH to CNDH. CVD: cardiovascular diseases; RD: respiratory diseases; COPD: chronic
 251 obstructive pulmonary disease.

252

253 Considering the nine key cities, total daily mortality increases from PRE-CNDH to CNDH except
 254 Shanghai, in which O₃ is slightly underestimated. Four megacities (Beijing, Shanghai, Wuhan and
 255 Guangzhou) with enormous populations have the highest daily deaths (24-28) during CNDH, 50% larger
 256 than the mean level (16) in the other 272 Chinese cities (Chen et al., 2018; Yin et al., 2017). It is worth
 257 noting that higher increase rate of daily mortality is found in tourist cities (Sanya and Changsha). In Sanya,
 258 daily deaths even increase by as high as 303% from PRE-CNDH to CNDH. An even higher increase in
 259 health risk may occur in Sanya if consider sharply increased tourists flow during CNDH.

260



261 **4. Conclusion and Implications**

262 In this study, we find the significant increase in O_3 during the CNDH throughout China especially
263 in the south part, which is attributed to the changes in precursor emissions, sensitivity regime, and the
264 enhanced regional transport. Moreover, the elevated O_3 also causes serious impacts on human health, with
265 total daily mortality from all non-accidental causes increasing from 151 to 201 in China. More
266 comprehensive studies should be conducted to better understand the long-holiday impacts (such as during
267 the CNDH) of O_3 in the future and here we suggest:

- 268 1) More strident emission control policies should be implemented in China before and during
269 CNDH to inhibit the elevated O_3 . And more localized control policies with the consideration of
270 the O_3 sensitivity regimes should be applied.
- 271 2) For reducing the health risk from the elevated O_3 , it is suggested to avoid travelling in rush hours
272 especially in midday during the CNDH.
- 273 3) Reducing the activities of private gasoline vehicles is effective to mitigate excess emissions
274 during the CNDH. It is encouraged to go out by electric car or public transportation such as bus,
275 subway and train.

276
277 *Acknowledgments.* This work was supported by the National Natural Science Foundation of China (Grant
278 No. 41530641/41673116/41961144029), the National Key Research and Development Program
279 (2017YFC02122802), Theme-based Research Scheme (No. T24-504/17-N), Youth Innovation Promotion
280 Association, CAS (2017406) and Guangdong Foundation for Program of Science and Technology Research
281 (Grant No. 2017B030314057).

282 *Author contributions.* PW and YZ designed the research. PW, JS, MX, SS and HZ analyzed the data. PW
283 performed air quality model. PW and YZ wrote the manuscript with comments from all co-authors.

284 *Competing interests.* The authors declare that they have no conflict of interest.

285 *Data availability.* The datasets used in the study can be accessed from websites listed in the references or
286 by contacting the corresponding author (zhang_yl86@gig.ac.cn).

287
288
289
290
291



292 References

- 293 Forecast report on travel index during Mid-Autumn Festival and National Day in 2018, 2018.
294 Anenberg, S. C., Horowitz, L. W., Tong, D. Q., and West, J. J.: An Estimate of the Global Burden of Anthropogenic
295 Ozone and Fine Particulate Matter on Premature Human Mortality Using Atmospheric Modeling, *Environmental*
296 *Health Perspectives*, 118, 1189-1195, 2010.
297 Brauer, M., Freedman, G., Frostad, J., Van Donkelaar, A., Martin, R. V., Dentener, F., Van Dingenen, R., Estep, K.,
298 Amini, H., and Apte, J. S.: Ambient Air Pollution Exposure Estimation for the Global Burden of Disease 2013,
299 *Environmental Science & Technology*, 50, 79-88, 2016.
300 Chen, K., Fiore, A. M., Chen, R., Jiang, L., Jones, B., Schneider, A., Peters, A., Bi, J., Kan, H., and Kinney, P. L.:
301 Future ozone-related acute excess mortality under climate and population change scenarios in China: A modeling
302 study, *PLOS Medicine*, 15, 2018.
303 Chen, P., Tan, P., Chou, C. C. K., Lin, Y., Chen, W., and Shiu, C.: Impacts of holiday characteristics and number of
304 vacation days on “holiday effect” in Taipei: Implications on ozone control strategies, *Atmospheric Environment*,
305 202, 357-369, 2019.
306 Cohan, D. S., Hakami, A., Hu, Y., and Russell, A. G.: Nonlinear response of ozone to emissions: source
307 apportionment and sensitivity analysis, *Environmental Science & Technology*, 39, 6739-6748, 2005.
308 Cohen, A. J., Anderson, H. R., Ostro, B., Pandey, K. D., Krzyzanowski, M., Künzli, N., Gutschmidt, K., Pope, A.,
309 Romieu, I., Samet, J. M., and Smith, K.: Urban air pollution, in: Comparative quantification of health risks, Global
310 and regional burden of disease attributable to selected major risk factors, Volume 1, World Health Organization,
311 Geneva, 2004.
312 Fang, X., Park, S., Saito, T., Tunnicliffe, R., Ganesan, A. L., Rigby, M., Li, S., Yokouchi, Y., Fraser, P. J., and
313 Harth, C. M.: Rapid increase in ozone-depleting chloroform emissions from China, *Nature Geoscience*, 12, 89-93,
314 2019.
315 Gao, J., Zhu, B., Xiao, H., Kang, H., Hou, X., and Shao, P.: A case study of surface ozone source apportionment
316 during a high concentration episode, under frequent shifting wind conditions over the Yangtze River Delta, China,
317 *Science of The Total Environment*, 544, 853-863, <https://doi.org/10.1016/j.scitotenv.2015.12.039>, 2016.
318 Gipson, G. L.: Chapter 16: Process analysis. In science algorithms of the EPA models-3 Community Multiscale Air
319 Quality (CMAQ) Modeling System. EPA/600/R-99/030, 1999.
320 Guenther, A. B., Jiang, X., Heald, C. L., Sakulyanontvittaya, T., Duhl, T., Emmons, L. K., and Wang, X.: The
321 Model of Emissions of Gases and Aerosols from Nature version 2.1 (MEGAN2.1): an extended and updated
322 framework for modeling biogenic emissions, *Geoscientific Model Development (GMD)*, 5, 1471-1492, 2012.
323 Hu, J., Chen, J., Ying, Q., and Zhang, H.: One-year simulation of ozone and particulate matter in China using
324 WRF/CMAQ modeling system, *Atmos. Chem. Phys.*, 16, 10333-10350, 10.5194/acp-16-10333-2016, 2016.
325 Huang, J., Pan, X., Guo, X., and Li, G.: Health impact of China's Air Pollution Prevention and Control Action Plan:
326 an analysis of national air quality monitoring and mortality data, *The Lancet Planetary Health*, 2, 2018.
327 Krewski, D., Jerrett, M., Burnett, R. T., Ma, R., Hughes, E., Shi, Y., Turner, M. C., Pope, C. A., 3rd, Thurston, G.,
328 Calle, E. E., Thun, M. J., Beckerman, B., DeLuca, P., Finkelstein, N., Ito, K., Moore, D. K., Newbold, K. B.,
329 Ramsay, T., Ross, Z., Shin, H., and Tempalski, B.: Extended follow-up and spatial analysis of the American Cancer
330 Society study linking particulate air pollution and mortality, *Res Rep Health Eff Inst*, 5-114; discussion 115-136,
331 2009.
332 Lelieveld, J., Barlas, C., Giannadaki, D., and Pozzer, A.: Model calculated global, regional and megacity premature
333 mortality due to air pollution, *Atmospheric Chemistry and Physics*, 13, 7023-7037, 2013.
334 Levy, I.: A national day with near zero emissions and its effect on primary and secondary pollutants, *Atmospheric*
335 *Environment*, 77, 202-212, <https://doi.org/10.1016/j.atmosenv.2013.05.005>, 2013.
336 Li, K., Jacob, D. J., Liao, H., Shen, L., Zhang, Q., and Bates, K. H.: Anthropogenic drivers of 2013–2017 trends in
337 summer surface ozone in China, *Proceedings of the National Academy of Sciences*, 116, 422-427,
338 10.1073/pnas.1812168116, 2019.
339 Li, M., Zhang, Q., Kurokawa, J. I., Woo, J. H., He, K., Lu, Z., Ohara, T., Song, Y., Streets, D. G., Carmichael, G.
340 R., Cheng, Y., Hong, C., Huo, H., Jiang, X., Kang, S., Liu, F., Su, H., and Zheng, B.: MIX: a mosaic Asian
341 anthropogenic emission inventory under the international collaboration framework of the MICS-Asia and HTAP,
342 *Atmos. Chem. Phys.*, 17, 935-963, 10.5194/acp-17-935-2017, 2017.
343 Li, T., Yan, M., Ma, W., Ban, J., Liu, T., Lin, H., and Liu, Z.: Short-term effects of multiple ozone metrics on daily
344 mortality in a megacity of China, *Environmental Science and Pollution Research*, 22, 8738-8746, 2015.



- 345 Li, Y., Lau, A. K. H., Fung, J. C. H., Zheng, J., Zhong, L., and Louie, P. K. K.: Ozone source apportionment
346 (OSAT) to differentiate local regional and super-regional source contributions in the Pearl River Delta region,
347 China, *Journal of Geophysical Research*, 117, 2012a.
- 348 Li, Y., Lau, A. K. H., Fung, J. C. H., Zheng, J. Y., Zhong, L. J., and Louie, P. K. K.: Ozone source apportionment
349 (OSAT) to differentiate local regional and super-regional source contributions in the Pearl River Delta region,
350 China, *Journal of Geophysical Research: Atmospheres*, 117, D15305, 10.1029/2011JD017340, 2012b.
- 351 Lim, S. S., Vos, T., Flaxman, A. D., Danaei, G., Shibuya, K., Adairrohani, H., Almazroa, M. A., Amann, M.,
352 Anderson, H. R., and Andrews, K. G.: A comparative risk assessment of burden of disease and injury attributable to
353 67 risk factors and risk factor clusters in 21 regions, 1990-2010: a systematic analysis for the Global Burden of
354 Disease Study 2010, *The Lancet*, 380, 2224-2260, 2012.
- 355 Liu, H., Liu, S., Xue, B., Lv, Z., Meng, Z., Yang, X., Xue, T., Yu, Q., and He, K.: Ground-level ozone pollution and
356 its health impacts in China, *Atmospheric Environment*, 173, 223-230,
357 <https://doi.org/10.1016/j.atmosenv.2017.11.014>, 2018a.
- 358 Liu, Y. H., Ma, J. L., Li, L., Lin, X. F., Xu, W. J., and Ding, H.: A high temporal-spatial vehicle emission inventory
359 based on detailed hourly traffic data in a medium-sized city of China, *Environ Pollut*, 236, 324-333,
360 10.1016/j.envpol.2018.01.068, 2018b.
- 361 Lu, X., Hong, J., Zhang, L., Cooper, O. R., Schultz, M. G., Xu, X., Wang, T., Gao, M., Zhao, Y., and Zhang, Y.:
362 Severe Surface Ozone Pollution in China: A Global Perspective, *Environmental Science & Technology Letters*, 5,
363 487-494, 10.1021/acs.estlett.8b00366, 2018.
- 364 National: National Health and Family Planning Commission of China,
365 <https://www.yearbookchina.com/navibooklist-n3018112802-1.html>, in, 2018.
- 366 National Bureau of Statistics of China: <http://www.stats.gov.cn/tjsj/pcsj/rkpc/6rp/indexch.htm>, 2010.
- 367 Pudasainee, D., Sapkota, B., Bhatnagar, A., Kim, S., and Seo, Y.: Influence of weekdays, weekends and bandhas on
368 surface ozone in Kathmandu valley, *Atmospheric Research*, 95, 150-156, 2010.
- 369 Sillman, S.: The use of NO_y, H₂O₂, and HNO₃ as indicators for ozone-NO_x-hydrocarbon sensitivity in urban
370 locations, *Journal of Geophysical Research: Atmospheres*, 100, 14175-14188, 10.1029/94jd02953, 1995.
- 371 Sillman, S., and He, D.: Some theoretical results concerning O₃-NO_x-VOC chemistry and NO_x-VOC indicators,
372 *Journal of Geophysical Research*, 107, 2002.
- 373 Streets, D. G., Bond, T. C., Carmichael, G. R., Fernandes, S. D., Fu, Q., He, D., Klimont, Z., Nelson, S. M., Tsai, N.
374 Y., Wang, M. Q., Woo, J. H., and Yarber, K. F.: An inventory of gaseous and primary aerosol emissions in Asia in
375 the year 2000, *Journal of Geophysical Research: Atmospheres*, 108, 10.1029/2002JD003093, 2003.
- 376 Tan, P.-H., Chou, C., and Chou, C. C. K.: Impact of urbanization on the air pollution "holiday effect" in Taiwan,
377 *Atmospheric Environment*, 70, 361-375, <https://doi.org/10.1016/j.atmosenv.2013.01.008>, 2013.
- 378 Tan, P., Chou, C., Liang, J., Chou, C. C. K., and Shiu, C.: Air pollution "holiday effect" resulting from the Chinese
379 New Year, *Atmospheric Environment*, 43, 2114-2124, 2009.
- 380 Wang, J., Ho, S. S. H., Cao, J., Huang, R., Zhou, J., Zhao, Y., Xu, H., Liu, S., Wang, G., Shen, Z., and Han, Y.:
381 Characteristics and major sources of carbonaceous aerosols in PM_{2.5} from Sanya, China, *Science of The Total
382 Environment*, 530-531, 110-119, <https://doi.org/10.1016/j.scitotenv.2015.05.005>, 2015.
- 383 Wang, P., Chen, Y., Hu, J., Zhang, H., and Ying, Q.: Source apportionment of summertime ozone in China using a
384 source-oriented chemical transport model, *Atmospheric Environment*, 211, 79-90,
385 <https://doi.org/10.1016/j.atmosenv.2019.05.006>, 2019a.
- 386 Wang, P., Chen, Y., Hu, J., Zhang, H., and Ying, Q.: Attribution of Tropospheric Ozone to NO_x and VOC
387 Emissions: Considering Ozone Formation in the Transition Regime, *Environmental Science & Technology*, 53,
388 1404-1412, 10.1021/acs.est.8b05981, 2019b.
- 389 Wang, P., Wang, T., and Ying, Q.: Regional source apportionment of summertime ozone and its precursors in the
390 megacities of Beijing and Shanghai using a source-oriented chemical transport model, *Atmospheric Environment*,
391 224, 117337, <https://doi.org/10.1016/j.atmosenv.2020.117337>, 2020a.
- 392 Wang, T., Xue, L., Brimblecombe, P., Lam, Y. F., Li, L., and Zhang, L.: Ozone pollution in China: A review of
393 concentrations, meteorological influences, chemical precursors, and effects, *Science of The Total Environment*, 575,
394 1582-1596, <https://doi.org/10.1016/j.scitotenv.2016.10.081>, 2017.
- 395 Wang, Y., Wild, O., Chen, X., Wu, Q., Gao, M., Chen, H., Qi, Y., and Wang, Z.: Health impacts of long-term ozone
396 exposure in China over 2013-2017, *Environment International*, 144, 106030,
397 <https://doi.org/10.1016/j.envint.2020.106030>, 2020b.
- 398 Wang, Z., Chen, Y., Su, J., Guo, Y., Zhao, Y., Tang, W., Zeng, C., and Chen, J.: Measurement and Prediction of
399 Regional Traffic Volume in Holidays, 2019 IEEE Intelligent Transportation Systems Conference, ITSC 2019,
400 2019c, 486-491.



401 Wiedinmyer, C., Akagi, S., Yokelson, R. J., Emmons, L., Al-Saadi, J., Orlando, J., and Soja, A.: The Fire INventory
402 from NCAR (FINN): a high resolution global model to estimate the emissions from open burning, *Geoscientific*
403 *Model Development*, 4, 625, 2011.

404 Xu, Z., Huang, X., Nie, W., Chi, X., Xu, Z., Zheng, L., Sun, P., and Ding, A.: Influence of synoptic condition and
405 holiday effects on VOCs and ozone production in the Yangtze River Delta region, China, *Atmospheric*
406 *Environment*, 168, 112-124, <https://doi.org/10.1016/j.atmosenv.2017.08.035>, 2017.

407 Yin, P., Chen, R., Wang, L., Meng, X., Liu, C., Niu, Y., Lin, Z., Liu, Y., Liu, J., and Qi, J.: Ambient Ozone
408 Pollution and Daily Mortality: A Nationwide Study in 272 Chinese Cities, *Environmental Health Perspectives*, 125,
409 117006, 2017.

410 Zhang, H., Li, J., Ying, Q., Yu, J. Z., Wu, D., Cheng, Y., He, K., and Jiang, J.: Source apportionment of PM_{2.5}
411 nitrate and sulfate in China using a source-oriented chemical transport model, *Atmospheric Environment*, 62, 228-
412 242, <https://doi.org/10.1016/j.atmosenv.2012.08.014>, 2012.

413 Zhang, Q., Streets, D. G., He, K., Wang, Y., Richter, A., Burrows, J. P., Uno, I., Jang, C. J., Chen, D., Yao, Z., and
414 Lei, Y.: NO_x emission trends for China, 1995–2004: The view from the ground and the view from space, *Journal of*
415 *Geophysical Research: Atmospheres*, 112, 10.1029/2007JD008684, 2007.

416 Zhao, J., Cui, J., Zhang, Y., and Luo, T.: Impact of holiday-free policy on traffic volume of freeway: An
417 investigation in Xi'an, in: 8th International Conference on Green Intelligent Transportation Systems and Safety,
418 2017, edited by: Wang, W., Jiang, X., and Bengler, K., Springer Verlag, 117-124, 2019.

419